

## Experimental demonstration of plasmonic Brewster angle extraordinary transmission through extreme subwavelength slit arrays in the microwave

N. Aközbeğ,<sup>1,\*</sup> N. Mattiucci,<sup>1</sup> D. de Ceglia,<sup>1</sup> R. Trimm,<sup>2</sup> A. Alù,<sup>3</sup> G. D'Aguanno,<sup>1</sup> M. A. Vincenti,<sup>1</sup> M. Scalora,<sup>4</sup> and M. J. Bloemer<sup>4</sup>

<sup>1</sup>*AEgis Technologies Inc., 410 Jan Davis Drive Huntsville, Alabama 35809, USA*

<sup>2</sup>*Miltec Corporation, 678 Discovery Drive, Huntsville, Alabama 35806, USA*

<sup>3</sup>*Department of Electrical and Computer Engineering, the University of Texas at Austin, Austin, Texas 78712, USA*

<sup>4</sup>*Department of the Army, C. M. Bowden Laboratory, Redstone Arsenal, Alabama 35898, USA*

(Received 2 October 2011; published 15 May 2012)

We experimentally demonstrate the existence of a Brewster-like broadband extraordinary optical transmission band, in a very thick metal plate with an array of slits as narrow as  $\lambda/750$  in the 8- to 40-GHz regime, by measuring the transmission from normal incidence to near grazing angles and mapping out the entire angular transmission spectrum. In the case of very narrow slits, an order of magnitude larger transmission is obtained at the Brewster angle when compared to the normal-incidence Fabry-Pérot resonance transmission peaks. Full-wave numerical simulations are in excellent agreement with the measurements, paving the way for the observation of this phenomenon in the optical regime.

DOI: [10.1103/PhysRevB.85.205430](https://doi.org/10.1103/PhysRevB.85.205430)

PACS number(s): 41.20.Jb, 42.25.Bs, 42.79.Dj, 78.20.Ci

Bulk metals are good reflectors ranging from optical frequencies to dc. However, opening an array of subwavelength apertures in an otherwise opaque metal screen can dramatically change their response at the subwavelength scale, leading to the generation of surface plasmons and extraordinary optical transmission (EOT). The demonstration of EOT through subwavelength apertures in metal screens<sup>1</sup> has stimulated great theoretical and experimental interest in understanding light interaction with corrugated metals, from the optical<sup>2</sup> to terahertz<sup>3</sup> and microwave frequencies.<sup>4</sup> There are a number of physical mechanisms that contribute to this phenomenon: in the case of one-dimensional (1D) metallic gratings, the extraordinary transmission can be attributed to plasmon excitation and cavity or Fabry-Pérot (FP) resonances for  $p$ -polarized incident radiation. While the angular dependence of extraordinary transmission and surface-wave generation has been analyzed both theoretically and experimentally, most studies have been limited to incidence angles below  $60^\circ$ , with the emphasis toward the plasmon wave dispersion relation. Recently, Alù *et al.* theoretically predicted a new extraordinary transmission phenomenon that, unlike cavity and plasmon resonances, which are frequency selective, is ultrabroadband but angular selective.<sup>5</sup> Independently, a similar phenomenon has also been predicted theoretically in the infrared based on spoof surface plasmon excitation, where a nearly flat high transmission band was predicted near grazing angles.<sup>6</sup> In Ref. 5, this effect has been associated with the equivalent of Brewster transmission for subwavelength gratings. In bulk lossless media, the Brewster angle is usually defined as the angle at which light is perfectly transmitted (zero reflection) for  $p$ -polarized radiation, satisfying the usual condition:  $\tan(\theta_B) = n$ , where  $n$  is the index of refraction.<sup>7</sup> In general, a simple closed form expression for the Brewster angle for lossy media is more difficult to define, but for metals a pseudo-Brewster angle may also be defined as  $\cos(\theta_B) = 1/|n|$ , at which absorption is maximum and reflectivity is minimum (but not zero).<sup>8</sup> At microwave frequencies, the minimum in the reflectivity of metals occurs at an angle of nearly  $90^\circ$

with a reflectivity of about 20%.<sup>9</sup> As described above, the introduction of periodic subwavelength slits in this type of metallic screen can restore perfect transmission and zero reflection for  $p$ -polarization at the *plasmonic Brewster angle*. In the limit of a perfect metal, each slit supports a transverse electromagnetic (TEM) mode, and the Brewster angle assumes the particularly simple condition:  $\cos \theta_B = w/d$ , where  $d$  is the grating period and  $w$  is the slit width.<sup>5</sup> This Brewster-like response holds true for an extremely wide range of frequencies, ranging from dc up to the frequency for which higher-order diffraction orders arise due to the grating periodicity. We also note that metallic gratings having narrow slits have been proposed as a metamaterial with a high index of refraction.<sup>10</sup> In this case, the subwavelength metal grating is replaced with a homogenous dielectric slab of effective refractive index  $n_{\text{eff}} = d/w$  and thickness  $l/n_{\text{eff}}$ , from which an effective Brewster angle follows from the standard definition for  $p$ -polarization, i.e.,  $\tan \theta_B = n_{\text{eff}} = d/w$ , consistent with the observation of a Brewster angle transmission band discussed in this paper.

In this paper, we experimentally demonstrate the existence of ultrabroadband Brewster-like transmission through a thick subwavelength metallic grating with slits much smaller than the incident wavelength ( $\lambda/750$ ) from X-band to Ka-band (8–40 GHz). At microwave frequencies, plasmonic effects arise inside these slits, due to their extreme subwavelength features, comparable with the metal skin depth. This proof-of-concept experiment may be, therefore, directly translated to infrared and optical wavelengths. Microwave measurements have been essential in the experimental demonstration and proof of concept of a number of important recent applications, such as photonic band-gap materials<sup>11</sup> and negative index metamaterials,<sup>12</sup> to pave the way to their realization in the optical regime.

Using an rf Agilent (E8363C) vector network analyzer, the zeroth diffraction order transmitted through the grating was measured from 8–40 GHz. Two set of linearly polarized horn antennas were used 8–18 GHz and 18–40 GHz. The experimental setup and a close-up sketch of the grating are

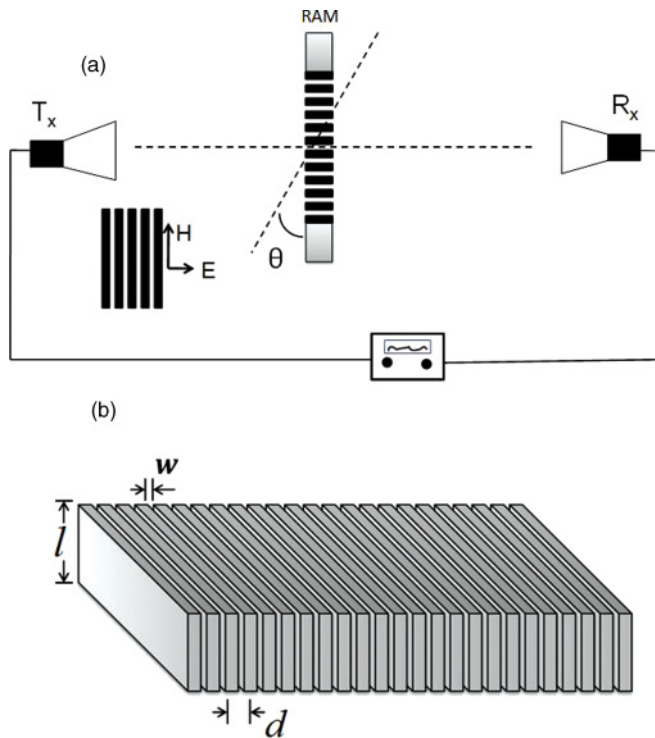


FIG. 1. (a) Sketch of the experimental setup and (b) geometry of the metal grating. Two identical rf horn antennas are used as  $T_x$  (emitter) and  $R_x$  (receiver), connected to a vector network analyzer. The grating is placed on a rotational stage, and transmission measurements are recorded from normal incidence ( $0^\circ$ ) to near grazing angles ( $85^\circ$ ).

shown in Fig. 1. The horn antennas were sufficiently placed away from the sample to ensure far-field radiation. However, due to the limitation of the testing area, perfect incident plane waves could not be achieved. The amplitude of the zeroth diffracted order was then measured by rotating the sample from  $0$  to  $85^\circ$ . Radar-absorbing material was wrapped around the sample to minimize any diffraction effects around the sample. The metallic grating was constructed using  $\sim 300$  extruded aluminum flat bars  $0.3175 \times 2.54$  cm. Spacers were used to achieve subwavelength slits as narrow as  $50 \mu\text{m}$ . The first grating was constructed using  $w = 1.5$  mm spacers with a grating period  $d = 4.7$  mm and the incident wavelength in the range  $0.75$  to  $3.75$  cm (frequency range  $8$ – $40$  GHz). The open area was approximately  $32\%$  with a slit size corresponding to  $\lambda/25$  at  $8$  GHz. The effective Brewster angle for these set of grating parameters is expected at  $\theta_B = \cos^{-1}(w/d) \cong 70^\circ$ .

Rayleigh-Woods anomalies,<sup>13,14</sup> arising at the onset of higher diffraction orders, are expected around  $64$  GHz at normal incidence. The measured transmission data in decibels as a function of angle of incidence is shown in Fig. 2(a). Calibration was done by taking a reference measurement without the sample. Here, the onset of the first diffraction order is cutting through the transmission bands above  $30$  GHz. Nevertheless, it can be seen that a high transmission band is obtained around  $70^\circ$  for all considered frequencies below  $30$  GHz, as expected. In Fig. 2(b) we show full-wave simulations based on the Fourier modal method (FMM)<sup>15</sup> for the same grating parameters, in excellent agreement with

our measurements, capturing all relevant underlying physical features. At normal incidence, high transmission bands are the results of cavity resonances, determined primarily by the FP resonances arising at frequencies  $\nu_N = Nc/2l$ ,  $N = 1, 2, \dots$  where  $c$  is the speed of light in vacuum. These transmission resonances are weakly affected by variations in the incidence angle up to  $60^\circ$ , and they dominate the transmission spectra of Fig. 2 as horizontal pass bands, with a transmission peak in the range of  $80\%$ . As the incidence angle is further increased, a new high transmission band is found around the expected plasmonic Brewster angle  $\sim 70^\circ$ , spanning the measured frequency range in perfect agreement with the theoretical predictions in Ref. 5, and producing a vertical passband with transmission levels above  $90\%$ . Measurements for  $s$ -polarization were performed to verify the polarization selectivity of this phenomenon and ensure that there was no radiation leakage around the sample, particularly at steeper angles. We find that at all frequencies and angles the transmission was less than  $-30$  dB for  $s$ -polarization. In addition, the grazing angle high transmission band was also verified by placing an aluminum foil at the back of the grating sample, where no high transmission was observed.

In order to show the dependence of the plasmonic Brewster angle on the filling ratio, we have constructed another grating with slit width  $w = 400 \mu\text{m}$  and period  $d = 3.2$  mm, resulting in a filling ratio of  $10\%$  and slit size on the order of  $\lambda/100$  at  $8$  GHz. In this case, the plasmonic Brewster angle is expected at around  $80^\circ$ . The measured transmission data is shown in Fig. 2(c), highlighting a clear vertical passband associated with the plasmonic Brewster angle. It is also evident that, as the slit size is narrowed, FP resonances become narrower with a higher contrast ratio, but the bandwidth of the Brewster transmission is not affected. Full-wave simulations shown in Fig. 2(d) are again in good agreement with the measurements.

An important question is how narrow can the slits be made and still realize a high transmission ultrabroad passband at the Brewster angle? At microwave frequencies, a metal is generally considered a perfect conductor, and metallic slits usually guide a TEM mode with wave number equal to the one of the material filling the slit (free-space here). However, this assumption is no longer valid when the slit size approaches the characteristic skin depth.<sup>16</sup> This skin effect is particularly relevant in terms of additional losses and absorption.

To verify this extreme scenario, we have constructed and measured a third grating with  $w = 50 \mu\text{m}$  ( $\lambda/750$  at  $8$  GHz), for which the filling ratio is only  $1.6\%$ . The corresponding transmission measurements are shown in Fig. 3(a). At normal incidence, the FP transmission bands are significantly affected when compared to the case with  $400\text{-}\mu\text{m}$  slits, since the skin depth plays a significant effect in this extreme scenario. Even here, however, Brewster-like transmission is verified with significantly higher levels of transmission ( $70\%$ ) than at FP resonances ( $6\%$ ), corresponding to an enhancement of an order of magnitude. The full-wave simulation, using COMSOL finite element software, taking into account the finite conductivity of aluminum, is shown in Fig. 3(b), which is in good agreement with the measurements. As the filling ratio becomes smaller, the angular spread of the Brewster transmission band becomes narrower as well and becomes very close to grazing angle. This makes it more difficult experimentally to resolve the Brewster

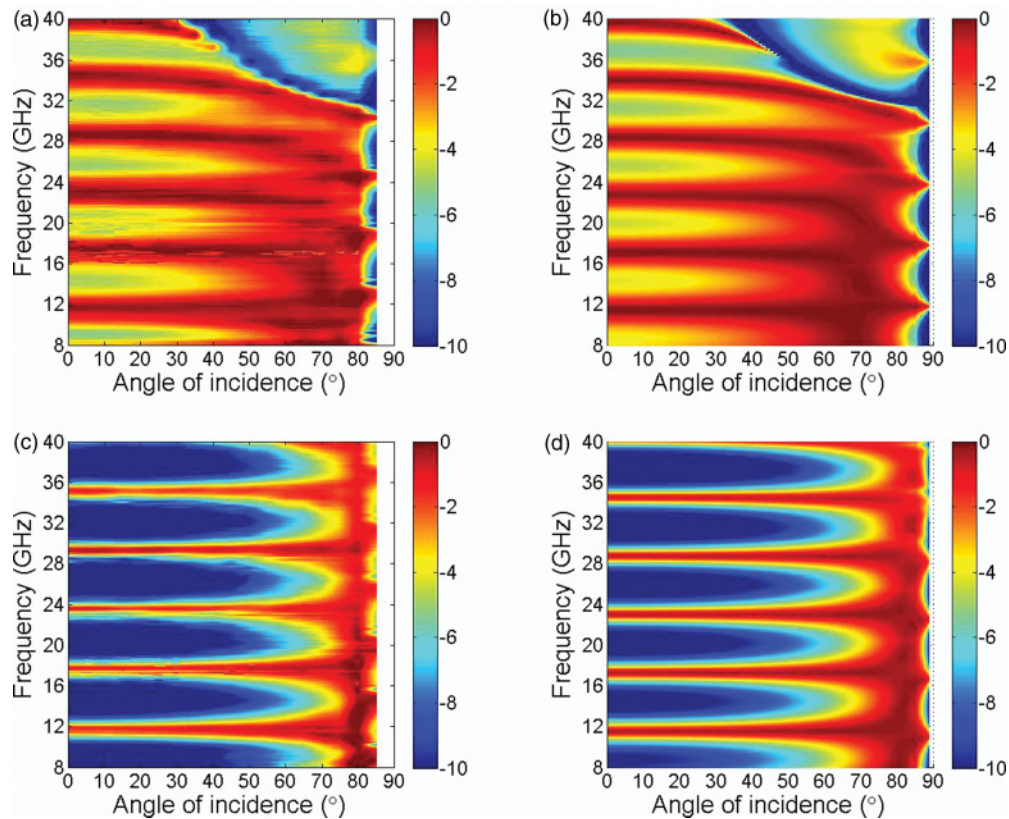


FIG. 2. (Color online) Measured transmission (in dB; left column) and full-wave simulations (right column) for a grating with (a) and (b)  $w = 1.5$  mm,  $d = 4.7$  mm, and open area  $w/d = 32\%$ ; (c) and (d)  $w = 400$   $\mu\text{m}$ ,  $d = 3.6$  mm, and  $w/d = 11\%$ . The grating thickness  $l = 2.54$  cm is the same in both cases. Nearly perfect transmission at the expected Brewster angle for (a) and (b)  $70^\circ$  and (c) and (d)  $80^\circ$  incidence confirms the dependence of the Brewster angle on the grating filling ratio. The measured and simulated data are in very good agreement.

angle band. Nevertheless, the vertical high transmission band at the Brewster angle is clearly seen spanning the entire frequency range. To further elucidate this result, we show in Fig. 4 the simulated absorbance spectrum, showing that at normal incidence, losses are quite significant ( $\sim 50\%$ ), due to the high Q factor of FP resonances in this extreme case, whereas at the Brewster angle a high transmission-band is preserved with minimal loss and reflection. This effect is a

symptom of the different physical mechanisms involved in classic EOT transmission and in Brewster-like anomalous transmission. In the first scenario, the field is transmitted building up in the steady state after a series of multiple reflections at the highly mismatched entrance and exit faces of the grating, which effectively form a resonant cavity. In contrast, Brewster-like transmission is achieved due to an anomalous impedance matching phenomenon, for which the

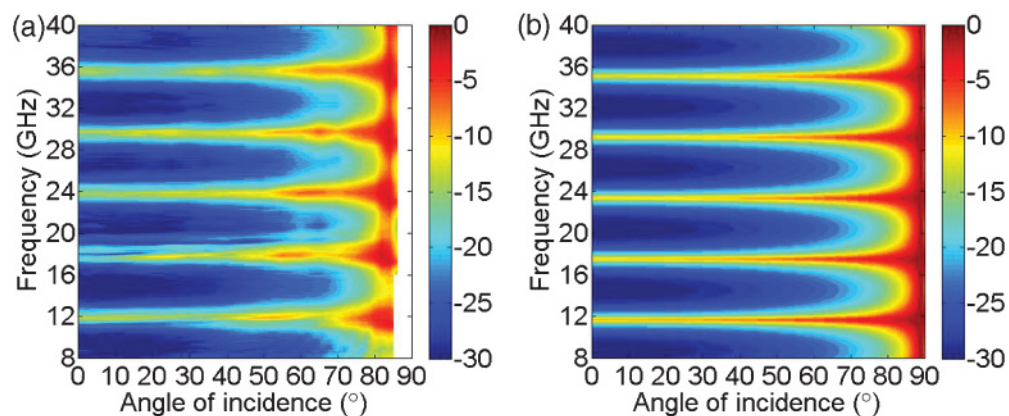


FIG. 3. (Color online) Transmission spectra (in dB) as a function of incident angle: (a) experiment and (b) full-wave simulations (COMSOL), for a subwavelength grating and slit size of  $50$   $\mu\text{m}$ , period  $3.2$  mm, and open area  $w/d = 1.6\%$ . The Brewster angle high transmission band is clearly seen when compared to the conventional FP resonances.

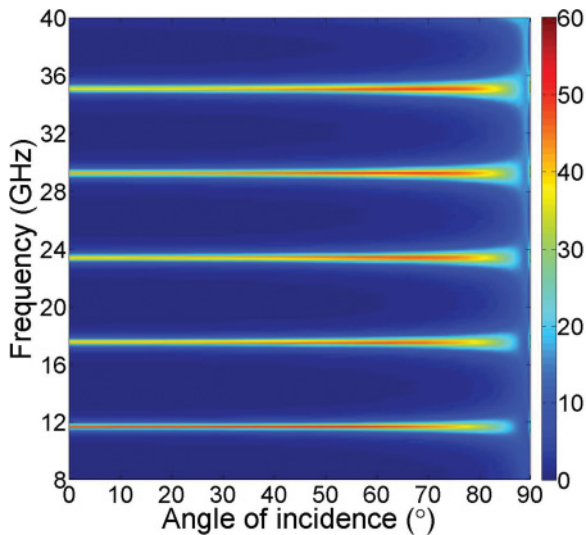


FIG. 4. (Color online) Full-wave simulated (COMSOL) percent-age absorbance for a grating with 50- $\mu\text{m}$  slit, consistent with Fig. 3. Significant absorption losses ( $\sim 50\%$ ) are clearly seen at the FP resonances, but minimal losses are obtained around the Brewster angle transmission band.

impinging wave, independent of the frequency of excitation, “feels” the same impedance in vacuum and inside the slits, avoiding any reflection at the entrance and exit faces of the grating, regardless of the grating thickness  $l$ .<sup>5</sup>

This feature is particularly relevant to realize efficient sensors and absorbers, as extracting energy from the system largely affects any resonant mechanism, like FP transmission, but would only weakly affect the Brewster-like matching phenomenon described here. The robustness of the Brewster transmission is particularly remarkable in our experimental

results, considering that stock aluminum bars were utilized, without polishing or special machining.

The existence of zeroth order broadband extraordinary transmission is valid as long as the incident wavelength is longer than the grating period, and it does not couple with higher-order diffraction orders. In principle, it is possible to extend the frequency band of the Brewster-like transmission from the rf to optical frequencies by reducing the period and the corresponding slit size.<sup>5</sup>

In conclusion, we have experimentally demonstrated a plasmonic Brewster effect, showing that a thick metal grating can exhibit ultrabroadband, nearly perfect transmission at the plasmonic Brewster angle. We have shown that, by changing the filling ratio of the grating, the Brewster angle can be tuned, allowing the possibility to engineer artificial materials with effective electromagnetic properties. In addition, we have shown that this ultrabroadband mechanism is much more robust to losses and absorption than regular resonant mechanisms for anomalous transmission. Excellent agreement with numerical simulations suggests that this phenomenon can be directly scaled to higher frequencies, including the optical regime, paving the way to new device applications based on ultrabroadband Brewster angle extraordinary transmission and light concentration. Radio-frequency and optical applications include broadband polarizers for polarimetric imaging, angular selective band pass filters, Brewster angle polarizers and windows for ultrashort pulses, and broadband energy concentrators. Following similar concepts, these results may also be relevant for grazing-angle infrared spectroscopy, as well as grazing-angle microscopy. We expect that these results can be extended to a two-dimensional geometry, for example, for an array of metallic tiles. While we have mainly discussed this phenomenon for electromagnetic waves, the recent demonstration of enhanced cavity-type transmission bands in 1D metal gratings in the acoustic regime<sup>17</sup> allows the possibility to extend the current results into acoustic regimes as well.

\*Corresponding author: neset.akozbek@us.army.mil

<sup>1</sup>T. W. Ebbesen, H. C. Lezec, H. F. Ghaemi, T. Thio, and P. A. Wolff, *Nature* **391**, 667 (1998).

<sup>2</sup>F. J. Garcia-Vidal, L. Martin-Moreno, T. W. Ebbesen, and T. Kuipers, *Rev. Mod. Phys.* **82**, 729 (2010).

<sup>3</sup>J. W. Lee, M. A. Seo, D. J. Park, S. C. Jeong, Q. H. Park, Ch. Lienau, and D. S. Kim, *Opt. Express* **14**, 12637 (2006).

<sup>4</sup>F. Yang and J. R. Sambles, *Phys. Rev. Lett.* **89**, 063901 (2002).

<sup>5</sup>A. Alù, G. D’Aguanno, N. Mattiucci, and M. J. Bloemer, *Phys. Rev. Lett.* **106**, 123902 (2011).

<sup>6</sup>X. R. Huang, R. W. Peng, and R. H. Fan, *Phys. Rev. Lett.* **105**, 243901 (2010).

<sup>7</sup>M. Born and E. Wolf, *Principles of Optics* (Pergamon Press, New York, 1980).

<sup>8</sup>B. Hüttner, *J. Appl. Phys.* **78**, 4799 (1995).

<sup>9</sup>I. R. Hooper, J. R. Sambles and A. P. Bassom, *Opt. Express* **16**, 7580 (2008).

<sup>10</sup>J. T. Shen, P. B. Catrysse, and S. Fan, *Phys. Rev. Lett.* **94**, 197401 (2005).

<sup>11</sup>E. Yablonovitch, T. J. Gmitter, and K. M. Leung, *Phys. Rev. Lett.* **67**, 2295 (1991).

<sup>12</sup>R. A. Shelby, D. R. Smith, and S. Shultz, *Science* **292**, 77 (2001).

<sup>13</sup>R. W. Wood, *Philos. Mag.* **4**, 396 (1902).

<sup>14</sup>O. M. Lord Rayleigh, *Proc. R. Soc. London Ser. A* **79**, 399 (1902).

<sup>15</sup>G. D’Aguanno, N. Mattiucci, M. J. Bloemer, D. de Ceglia, M. A. Vincenti, and A. Alu, *J. Opt. Soc. Am. B* **28**, 253 (2011).

<sup>16</sup>J. R. Suckling, A. P. Hibbins, M. J. Lockyear, T. W. Preist, J. R. Sambles, and C. R. Lawrence *Phys. Rev. Lett.* **92**, 147401 (2004).

<sup>17</sup>Ming-Hui Lu, X. K. Liu, L. Feng, J. Li, C. P. Huang, Y. F. Chen, Y. Y. Zhu, S. N. Zhu, and N. B. Ming, *Phys. Rev. Lett.* **99**, 174301 (2007).